A flow bioreactor system compatible with real-time two-photon fluorescence lifetime imaging microscopy

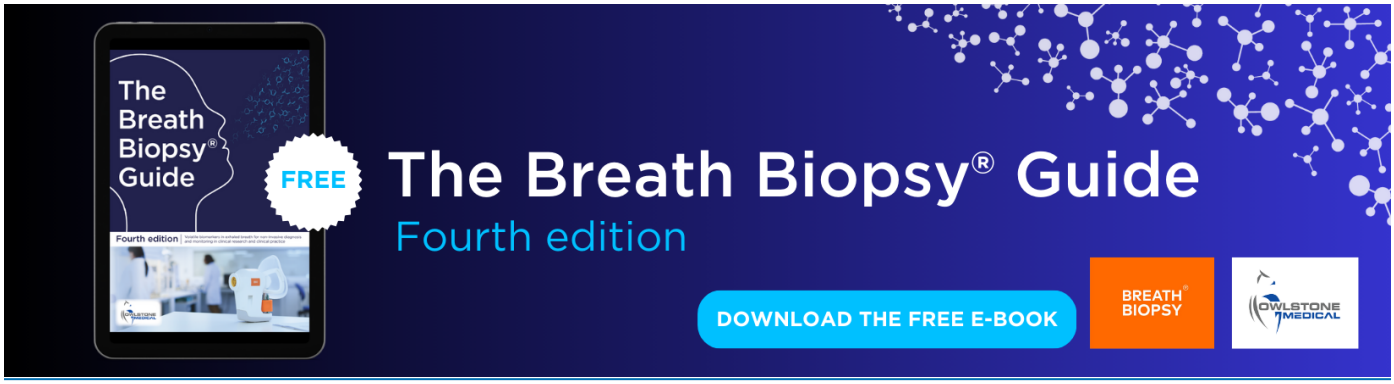

Biomedical Materials

PAPER

A flow bioreactor system compatible with real-time two-photon fluorescence lifetime imaging microscopy

Nian Shen[1,2,8], **Julia A Riedl**[1,2,3,8], **Daniel A Carvajal Berrio**[1], **Zachary Davis**[1,4], **Michael G Monaghan**[1,5,6], **Shannon L Layland**[1,2], **Svenja Hinderer**[1,2] and **Katja Schenke-Layland**[1,2,7,9]

[1] Department of Women's Health, Research Institute of Women's Health, University Hospital of the Eberhard Karls University, Tübingen, Germany
[2] Department of Cell and Tissue Engineering, Fraunhofer Institute for Interfacial Engineering and Biotechnology IGB, Stuttgart, Germany
[3] Medical Scientist Training Program (MD/PhD), University of Minnesota Medical School, Minneapolis, MN, United States of America
[4] Department of Material Science and Engineering, North Carolina State University, Raleigh, NC, United States of America
[5] Trinity Centre for Bioengineering, Trinity College Dublin, Dublin, Ireland
[6] Department of Mechanical & Manufacturing Engineering, Trinity College Dublin, Dublin, Ireland
[7] Department of Medicine/Cardiology, CVRL, David School of Medicine at UCLA, Los Angeles, CA, United States of America
[8] These authors contributed equally to this work.
[9] Author to whom any correspondence should be addressed.

E-mail: nian.shen@med.uni-tuebingen.de, brekk129@umn.edu, Daniel.Carvajal-Berrio@med.uni-tuebingen.de, zgdavis@ncsu.edu, MONAGHMI@tcd.ie, shannon.layland@igb.fraunhofer.de, svenja.hinderer@igb.fraunhofer.de and katja.schenke-layland@med.uni-tuebingen.de

OPEN ACCESS

RECEIVED
30 July 2017

REVISED
31 October 2017

ACCEPTED FOR PUBLICATION
17 November 2017

PUBLISHED
1 February 2018

Keywords: FLIM, HUVEC, multiphoton imaging, endothelial cells, 3D cell culture, 2P-FLIM

Supplementary material for this article is available online

Abstract

Bioreactors are essential cell and tissue culture tools that allow the introduction of biophysical signals into *in vitro* cultures. One major limitation is the need to interrupt experiments and sacrifice samples at certain time points for analyses. To address this issue, we designed a bioreactor that combines high-resolution contact-free imaging and continuous flow in a closed system that is compatible with various types of microscopes. The high throughput fluid flow bioreactor was combined with two-photon fluorescence lifetime imaging microscopy (2P-FLIM) and validated. The hydrodynamics of the bioreactor chamber were characterized using COMSOL. The simulation of shear stress indicated that the bioreactor system provides homogeneous and reproducible flow conditions. The designed bioreactor was used to investigate the effects of low shear stress on human umbilical vein endothelial cells (HUVECs). In a scratch assay, we observed decreased migration of HUVECs under shear stress conditions. Furthermore, metabolic activity shifts from glycolysis to oxidative phosphorylation-dependent mechanisms in HUVECs cultured under low shear stress conditions were detected using 2P-FLIM. Future applications for this bioreactor range from observing cell fate development in real-time to monitoring the environmental effects on cells or metabolic changes due to drug applications.

Introduction

Fluid shear stress, due to blood flow through vessels, plays a crucial role in angiogenesis [1], cell proliferation [2], migration [3], differentiation [2, 4], and metabolism [5]. Cells are sensitive to shear stress, which can ultimately alter cell function through activation of mechanosensitive molecules involved in cell signaling pathways [6]. Bioreactor systems are commonly closed systems that employ mechanical stimuli to cells and *in vitro*-generated cell-based three-dimensional (3D) tissues with the goal to mimic *in vivo* physiological conditions [7]. Depending on the type of cell or tissue, parameters such as temperature, oxygen concentration, mechanical and electrical stimulation [8] are the typically manipulated and monitored in bioreactor systems. One limitation of the majority of the currently existing bioreactor systems is the need to interrupt the culture at defined time points to gather information about the status of the sample using invasive methods. High-resolution optical techniques such as Raman microspectroscopy and near-infrared

two-photon fluorescence lifetime imaging microscopy (2P-FLIM) are widely used to detect cell phenotypic changes, metabolic activity, and protein expression of cells without the need for exogenous markers [9–11]. It would be highly advantageous to develop a bioreactor system that allows real-time high-resolution imaging of cells and tissues that are exposed to biomechanical stress *in vitro* without the need to stop the experiment or sacrifice the sample. However, to combine high-resolution imaging modalities with continuous flow bioreactor systems is challenging due to short working distances and constraints of optical transparency. Although some custom-built and commercially available devices have been developed to apply shear stress *in vitro*, few existing designs are optimized to allow for simultaneous high-resolution live-cell microscopy [4, 12, 13]. Microfluidic devices were designed for high-resolution live-cell microscopy. However, these devices also face technical challenges [14]. For example, bubbles in the microfluidic channels/chambers are difficult to remove and may damage cells, therefore hindering the control of these devices [14]. Furthermore, unlike bioreactor systems, microfluidic devices are designed to culture and analyze single cells or monolayers of cells, but they are not suitable for the culture of larger samples such as 3D tissues [14].

Here, we present a bioreactor that combines high-resolution contact-free imaging and continuous flow in a closed system that is compatible with various types of microscopes. 2P-FLIM has recently emerged in the field biology as a tool to study complex biological samples [15–17]. It is a non-invasive method that relies on the principle that intrinsic molecules within cells, such as amino acids, proteins, and lipids often emit a well-perceivable fluorescence after excitation with light in the ultraviolet or visible range [18]. This excitation is accomplished using near-infrared femtosecond multi-photon lasers. Therefore, no exogenous fluorescent dyes must be added to the culture for visualization and analysis. In addition to cellular and tissue autofluorescence, 2P-FLIM can detect pH level, cation (Ca^{2+}, Mg^{+}, K^{+}) concentration, oxygen concentration and fluorescence resonant energy transfer [19–23]. NAD(P)H (nicotinamide adenine dinucleotide (phosphate)) is a key enzyme involved in glycolysis and oxidative phosphorylation [11, 23, 24]. Changes of NAD(P)H and FAD (flavin adenine dinucleotide) are reflective of cellular metabolism [25] that can be non-invasively detected with 2P-FLIM. Shear stress has been shown to influence metabolic activity and migration of endothelial cells [26], therefore, we aimed to investigate the influence of shear stress on cell migration, cell metabolism and apoptosis of human umbilical vein endothelial cells (HUVECs) by implementing bright field imaging and 2P-FLIM in our bioreactor system.

Materials and methods

Cell culture

HUVECs were obtained from Lonza (CC-2517, Basal, Switzerland). Passages 3–6 were used for all experiments with the corresponding EBM-2 MV BulletKit medium (CC-3156 and CC-4147; Lonza).

For the bioreactor experiments, HUVECs were trypsinized (0.25% trypsin-EDTA) and re-seeded at a density of 3×10^4 cells cm^{-2} on circular 25 mm diameter coverslips (Nunc Thermanox, Thermo Fischer Scientific, Langselbold, Germany). The cell-seeded coverslips were cultured overnight in a six-well plate at 37 °C and 5% CO_2 to allow cell attachment prior transfer into the bioreactor system.

Imaging bioreactor system

A custom-built, autoclavable imaging bioreactor system was designed using Solidworks (Solidworks2010, Dassault Systemes SolidWorks Corporation, Ludwigsburg, Germany) (figure 1). A computational model was developed to assess the performance of the bioreactor system in silico. Meshing and calculations were performed in COMSOL 4.3a based on the bioreactor geometry and dimensions (COMSOL Multiphysics GmbH, Berlin, Germany). The medium was considered as an incompressive Newtonian fluid. Therefore, the equation used in the simulation was incompressive Navier–Stokes equations as follows (equations (1) and (2)):

$$\nabla \cdot \mathbf{v} = \mathbf{0} \tag{1}$$

$$\rho\left(\frac{\partial}{\partial t}\mathbf{u}\right) + \rho(\mathbf{u} \cdot \nabla)\mathbf{u} = \nabla \cdot (-p\mathbf{I} + \mu(\nabla\mathbf{u} + (\nabla\mathbf{u})^T)), \tag{2}$$

where $\mathbf{u}$ is the fluid velocity, ρ is the fluid density, $\mathbf{p}$ is the fluid pressure, μ is the fluid dynamic viscosity of the culture medium and $\mathbf{F}$ is the volume forces vector. The numerical values of the model parameters used in the simulations are displayed in table 1.

The bioreactor system consists of three parts: a transparent chamber top (made of polycarbonate), a flow chamber block and a bottom (both made of polyether-ether-ketone) (figure 1(a)). For all experiments, cell-seeded coverslips were placed between the flow chamber block and bottom. There are four fluidic chambers; each with a distinct inlet and outlet valve to enable laminar flow. Each fluidic chamber was connected to a closed tubing system (Ismatec, Wertheim-Mondfeld, Germany) containing a 30 ml medium reservoir (Schott AG, Mainz, Germany) and a filter with a 20 μm pore size (Whatman GmbH, Dassel, Germany). The cell medium was pumped from the reservoir through the system using a peristaltic pump with a CA8 pump head and cassette (Ismatec). All *in vitro* experiments were performed at 37 °C and 5% CO_2.

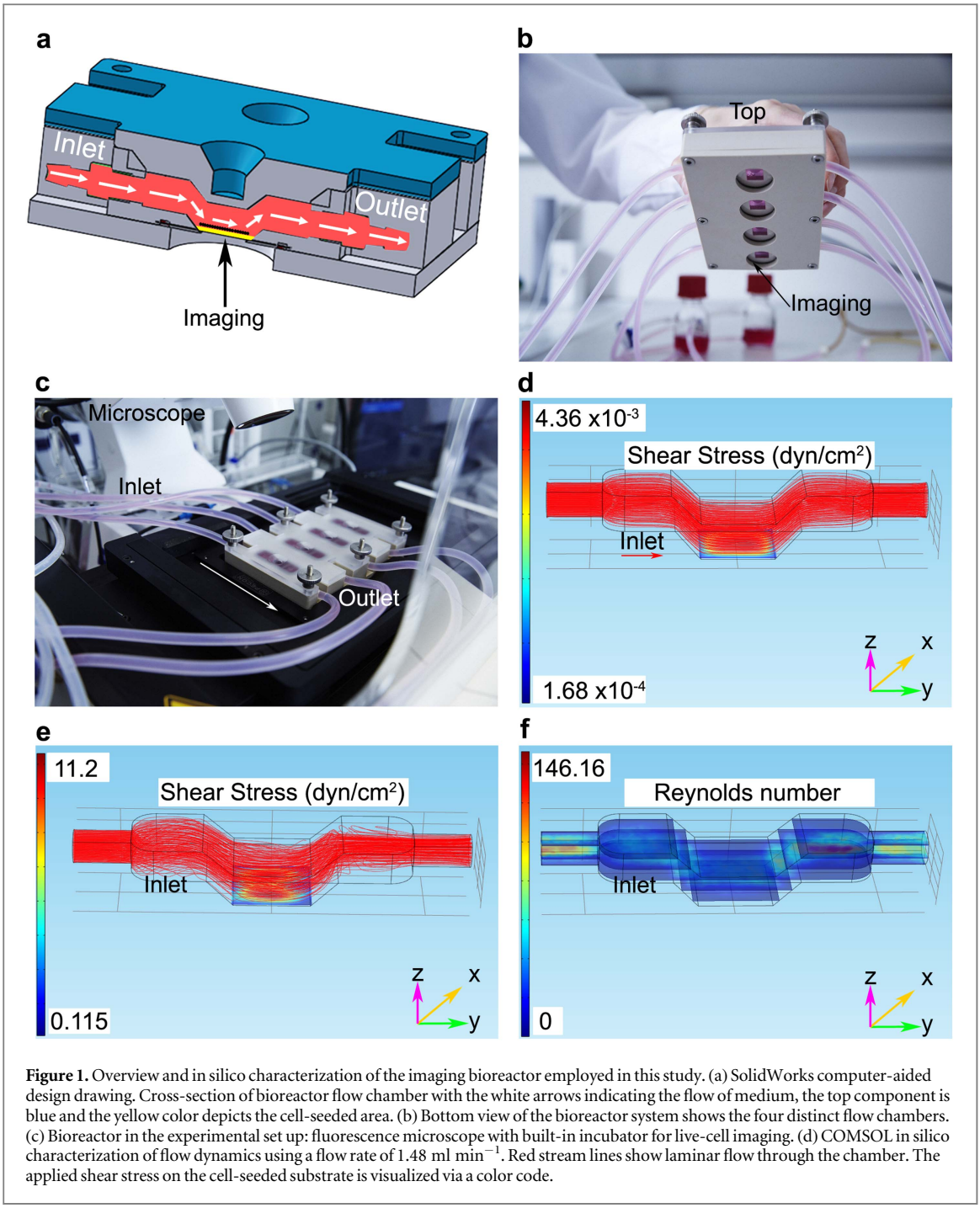

Figure 1. Overview and in silico characterization of the imaging bioreactor employed in this study. (a) SolidWorks computer-aided design drawing. Cross-section of bioreactor flow chamber with the white arrows indicating the flow of medium, the top component is blue and the yellow color depicts the cell-seeded area. (b) Bottom view of the bioreactor system shows the four distinct flow chambers. (c) Bioreactor in the experimental set up: fluorescence microscope with built-in incubator for live-cell imaging. (d) COMSOL in silico characterization of flow dynamics using a flow rate of 1.48 ml min^{-1}. Red stream lines show laminar flow through the chamber. The applied shear stress on the cell-seeded substrate is visualized via a color code.

Table 1. Numerical values of the model parameters used for the simulation.

Parameters (units)	Value	Reference
Inlet velocity	0	
Outlet pressure (Pa)	0	
Boundaries	No slip	
Fluid viscosity (Pa s)	8.1×10^{-4}	[51, 52]
Fluid density at 37 °C	10^3	[51, 52]
Temperature (K)	310.15	[51, 52]

Live-cell bright field microscopy

After 24 h of static cell culture, a p100 pipette tip (Eppendorf, Hamburg, Germany) was used to create a scratch and then coverslips were placed in the bioreactor system, with the scratch perpendicular to flow direction, medium was added, the closed system was connected to the medium pump and placed on the microscope stage for live-cell and 2P-FLIM data acquisition.

In this study, we utilized a Zeis AxioObserver Z1 (Carl Zeiss GmbH, Jena, Germany) with live-cell imaging compatibility and an attached, closed incubator to ensure 37 °C and 5% CO_2 during the entire experiment (figure 1(c)). A bright-field imaging channel and a 40× water immersion objective (N.A 1.1, Carl Zeiss GmbH) were used to acquire images every 5 min for

20 h after initial injury. The focus was set and fixed prior to the experiment.

Immunofluorescence and live/dead cell staining

After 24 h of culture within the bioreactor system, the cell-seeded coverslips were extracted from the bioreactor, fixed with 4% paraformaldehyde for 15 min, washed and then stained for the endothelial cell marker CD31 as described previously in detail [24]. Cell nuclei were visualized using 4′, 6-Diamidin-2-phenylindol (DAPI). Mouse IgG1 PECAM 1 (CD31; sc-71872, 1:100; Santa Cruz, Heidelberg, Germany) served as the primary antibody, and anti-mouse-IgG1-Alexa Fluor 594 (A-11005, 1:250; Life Technologies, Carlsbad, USA) was used as the secondary antibody. A confocal microscope LSM710 (Carl Zeiss GmbH) was used to obtain the images, which were processed using Photoshop CS3 (Adobe Systems, San Jose, USA).

To further characterize the bioreactor system, cell viability following a 24 h dynamic culture was assessed using a live/dead staining protocol. Fluorescein diacetate (FDA; Sigma-Aldrich, Darmstadt, Germany) at a concentration of 1 μg ml^{-1} and propidium iodide (PI; Sigma-Aldrich) at a concentration of 1 μg ml^{-1} were used. Dilutions were prepared with cell culture medium without fetal calf serum. For staining, the cells were washed with PBS and incubated for 15 min in the dark at 37 °C with the dye solution. The dye was then removed, the cells were washed with PBS and images were immediately acquired.

Two-photon fluorescence lifetime imaging microscopy (2P-FLIM)

2P-FLIM measurements were performed on a custom-made multiphoton laser system (JenLab GmbH, Jena, Germany) that has been previously described in detail [11, 25]. Two-photon excitation was generated using a Ti:Sapphire femtosecond laser (MaiTai XF1 Spectra Physics, United States, Santa Clara). The following settings were maintained for all 2P-FLIM experiments: multiphoton images were collected in the region of interest with a total acquisition time of 23 s, a laser power of 25 mW and a wavelength of 710 nm. Afterwards, the microscope was switched to 2P-FLIM mode for the acquisition of the decay data. All recording settings were adjusted using the software SPCM (Becker & Hickl GmbH, Berlin, Germany). Each 2P-FLIM measurement had a total recording time of 180 s and was controlled through the SPCM software (Becker & Hickl GmbH). Instrumental response function (IRF) was considered to acquire accurate results [26, 27]. The measurement of IRF was performed as previously described [28]. In detail, amorphous urea (Sigma-Aldrich) was dissolved in distilled water and added to a glass bottom dish (ibidi GmbH, Martinsried, Germany). After resting overnight, the water was evaporated, and the saturated concentration of urea formed crystals on the glass surface. Urea crystals were then measured to acquire the time-resolved scattering signal coming from the crystals. The excitation wavelength was 920 nm and acquisition time was 180 s with a laser power of 5 mW.

2P-FLIM data analysis

It is known that fluorescence signals originating from NAD(P)H contain contributions from free and protein-bound NAD(P)H [29]. Biexponential decay fitting was used to calculate the short and long lifetime components (τ_1 and τ_2, respectively), which mostly correspond to free and protein-bound NAD(P)H [30]. The relative contributions of the lifetime components (α_1 and α_2, where $\alpha_1 + \alpha_2 = 100\%$) were also calculated. The IRF was recorded from urea crystals, and the instrumental delays were taken into account in the lifetime calculations as previously described [11]. At the end of every fitting, χ^2, a parameter expressing the quality and accuracy of the biexponential decay fitting, was calculated. The fitting parameters were reevaluated until the average χ^2 per image was lower than 1.1. Every pixel was independently calculated to enable false color-coding based on the values of the different parameters (τ, α, and χ^2). Afterwards, every decay map pixel (2P-FLIM image) was exported as a text file and analyzed using ImageJ (freely available from www.nih.org). All data analyses were performed with the software SPCM (Becker & Hickl GmbH) with a binning factor of 6 and a threshold of approximately 30% of the maximum signal.

Statistical analysis

Normal data distribution was assessed using a Shapiro–Wilk test. For statistical analysis, the commercially available program GraphPad Prism 6 was used (GraphPad Software, Inc., La Jolla, CA). Students t-test was performed, and $p < 0.05$ was considered statistically significant.

Results

The imaging bioreactor system was designed and fabricated to allow cell and tissue cultures to be exposed to defined fluid shear stress while enabling high-resolution imaging (figure 1(a)). It has the same dimension as a typical cell culture plate (127 mm × 85 mm × 21 mm) making it compatible with various existing microscope systems. The bioreactor has four distinct flow chambers with no communication or connection between the chambers (figure 1(b)), enabling the execution of four independent experiments simultaneously. The transparent top component allows bright field light penetration and is suitable for inverted light microscopes. Windows were designed in the bottom component to ensure contact between the imaging objective and the cell-seeded area within the bioreactor system to allow for high-resolution imaging (figure 1(c)). In our proof-of-concept

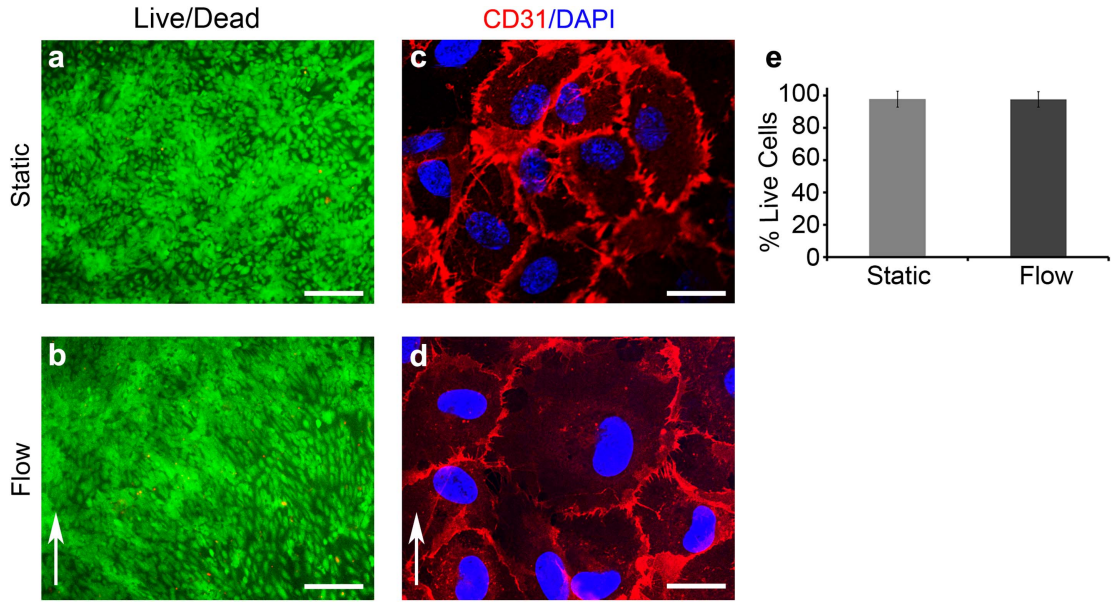

Figure 2. Fluorescence staining results 24 h after scratch assay under either static (a), (c) or dynamic (b), (d) conditions. (a), (b) Live/dead assay: living cells are stained in green and dead cells are visualized in red. Scale bars equal 100 μm. (c), (d) CD31 immunofluorescence staining (red) and DAPI (blue). Scale bars equal 20 μm. (e) Quantification of the live/dead assay from $n = 3$ images of both static and flow conditions. Error bars represent the standard deviation. There was no statistically significant difference between the two conditions.

experiment, cell-seeded coverslips were placed between the chamber block and bottom, with an O-ring seal. The coverslips are removable from the bioreactor system for end-point biological analysis. To characterize the dynamics of the flow chamber, simulations were performed using a computational simulation COMSOL. We simulated steady/state flow patterns within the fluidic chamber under the assumption of a fully-developed flow. As shown in figure 1(d), a constant shear stress between 1.69×10^{-4} and 4.36×10^{-3} dyn cm^{-2} was applied over the entire cell-seeded coverslip with a flow rate of 1.48 ml min^{-1}. The red streamlines confirmed a laminar flow of medium through the chamber. We identified 47 ml s^{-1} as the maximum flow rate to ensure laminar flow to the cells (figure 1(e)). With this flow rate, cell-seeded coverslips were subjected to a shear stress up to 11.2 dyn cm^{-2}. Here, the Reynolds number was lower than 2300, confirming laminar flow conditions in the bioreactor (figure 1(f)).

To assess the biocompatibility of the bioreactor system, HUVECs were dynamically cultured for 24 h at a flow rate of 1.48 ml min^{-1}. Cell viability was detected with a live/dead assay. As shown in figures 2(a), (b) and figure S1 is available online at stacks.iop.org/BMM/13/024101/mmedia, HUVECs cultured under static or flow conditions after 24 h retained viability (static: $97.4 \pm 0.01\%$ and bioreactor: $96.2 \pm 0.015\%$). No significant difference in the number of viable cells was detected between static and flow conditions (figure 2(e), $p > 0.05$). HUVECs in both conditions were CD31-positive, indicating that the phenotype of the cells was maintained (figures 2(c), (d)).

To demonstrate functionality of the bioreactor, HUVECs were subjected to a wound healing assay (scratch assay) similar to previous studies [31] and monitored in real-time (figure 3(a)). Interestingly, HUVECs under static conditions proliferated faster (a confluent monolayer was seen within 14 h) when compared with the cells that were subjected to flow (confluence was reached after 18 h) (figure 3(b)). We observed that similar to static cultures, HUVECs cultured with exposure to a flow rate of 1.48 ml min^{-1} showed a round morphology and did not align (figure S2).

We performed 2P-FLIM to analyze the cells under static and flow conditions in real-time in the bioreactor. The fluorescence decay curves for NAD(P)H were the best fit to a double exponential decay model, indicating the presence of two distinctly different lifetimes for the free and protein-bound forms of this coenzyme. The lifetimes of the free NAD(P)H (τ_1), and protein-bound NAD(P)H (τ_2), and the relative amplitude of free NAD(P)H (α_1) of HUVECs cultured under different conditions are displayed as false color-coded 2P-FLIM images in figure 4. Based on these images, histograms of α_1 of HUVECs cultured under different conditions were calculated (figure 5(a)). As indicated in figures 5(a), (b), α_1 and τ_1 of the 24 h laminar-sheared HUVECs were decreased when compared with the initial state (flow condition, 0 h). In contrast, α_1 in HUVECs cultured under static conditions showed similar lifetime distributions after 24 h of culture when compared to the initial state. An increased τ_2 was detected in the 24 h laminar-sheared

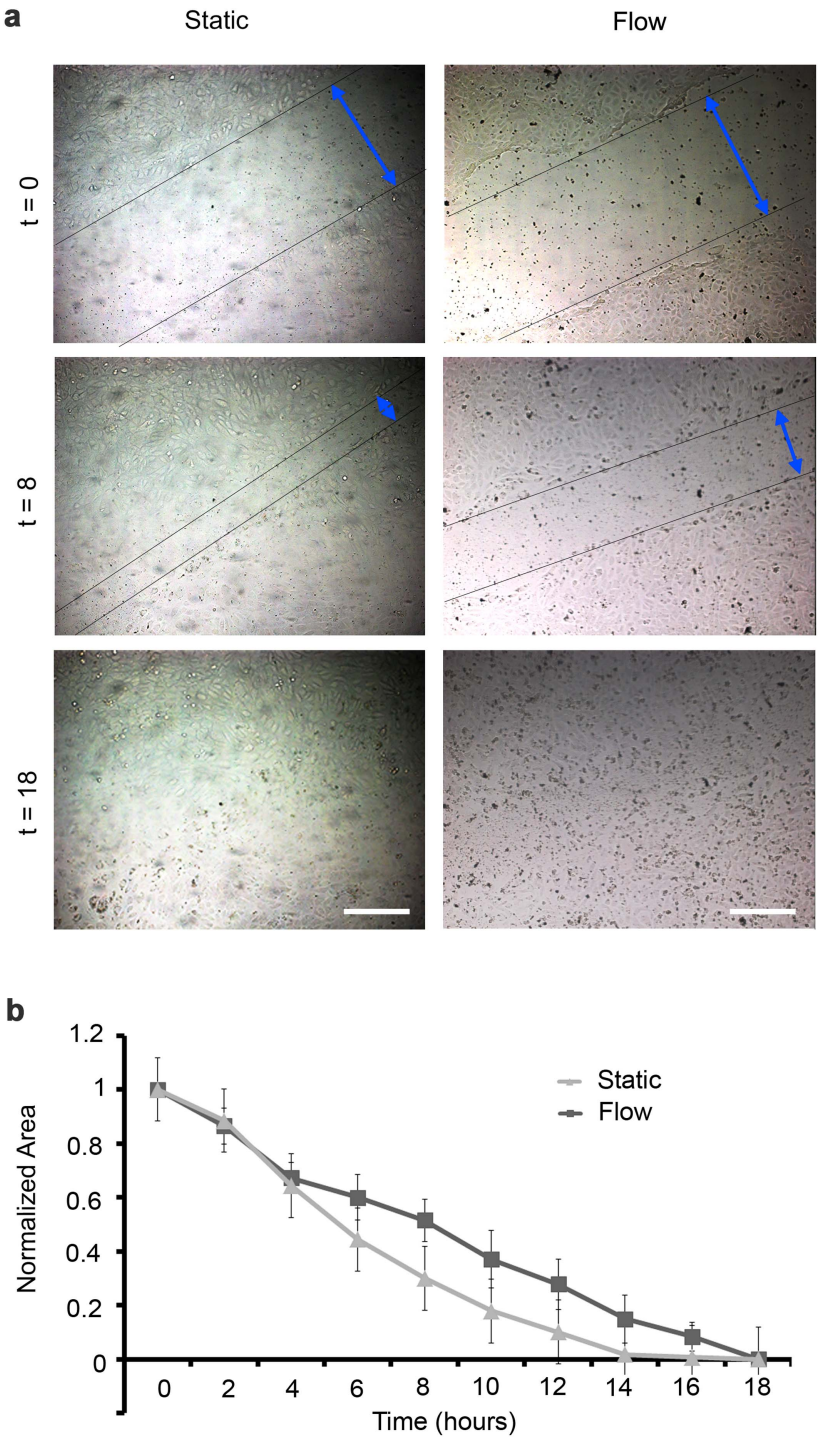

Figure 3. (a) Bright field images of HUVECs in the bioreactor during live-cell imaging. The black lines trace out the scratch area. The blue arrows show the scratch channels. Scale bars equal 100 μm. (b) Quantification of the reduction of scratch area over time for both static and flow conditions (each $n = 3$). Error bars represent the standard deviation.

HUVECs when compared to the cells prior exposure to defined shear (figure 5(c)).

Discussion

Bioreactor systems are widely used to mimic physiological conditions in cell and tissue cultures, and to specifically impact cellular behavior such as cell migration, proliferation, and phenotype maintenance [32]. However, many bioreactors do not permit *in situ* imaging and analyses [33, 34]. As a result, the sample must be removed from the bioreactor system and be prepared for further assessment. Thus, it is not possible to continuously monitor the culture and obtain data at several time points. Devices exist to support continuous low-resolution visualization of cells during flow, or high-resolution visualization of cells while stretching the

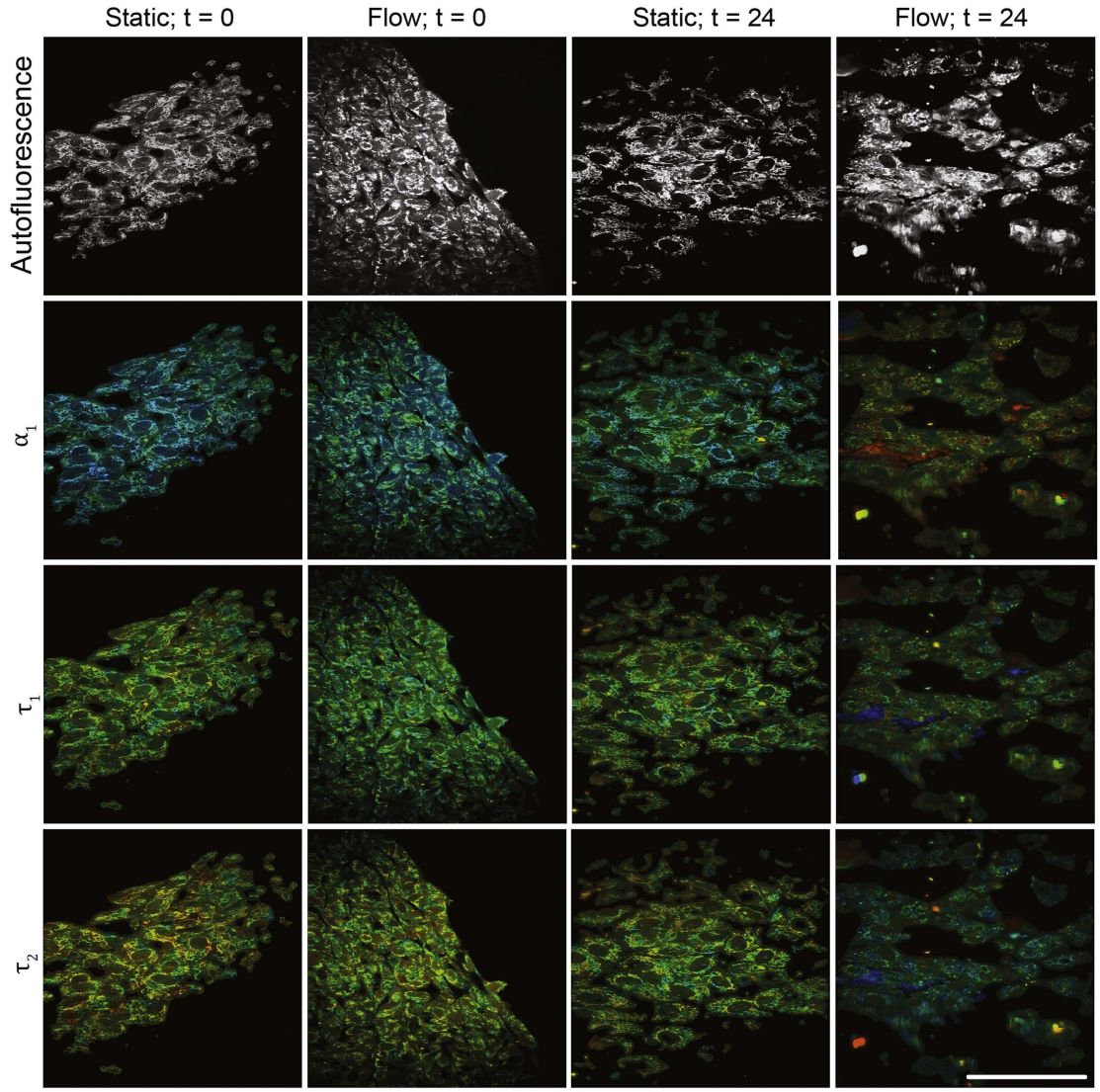

α_1 [%]	50% - 60%	60% - 70%	70% - 80%	80% - 90%
τ_1 [ns]	0.300 - 0.375	0.375 - 0.450	0.450 - 0.525	0.525 - 0.600
τ_2 [ns]	1.650 - 1.963	1.963 - 2.275	2.275 - 2.588	2.588 - 2.900

Figure 4. Multiphoton laser-induced autofluorescence images and false color-coded images of the relative contribution of free NAD(P)H (α_1) in HUVECs cultured under static or flow conditions. Scale bar indicates 100 μm.

substrate [35–39]. Nevertheless, high-resolution imaging of intracellular structural dynamics during shear stress applications is not readily feasible.

Here, we present a high throughput bioreactor system that is designed for real-time high-resolution imaging of cells and tissues that are exposed to fluid shear stress. To our knowledge, this is the first demonstration of combining a flow bioreactor system with 2P-FLIM. The windows at the bottom of the bioreactor allowed easy assembly onto the stage of a standard inverted light microscope system without interferences with the optical setup. The newly designed bioreactor system combines four independent flow chambers that allow the assessment of distinct culture conditions simultaneously and thereby largely improves the culture efficiency. The simulation of shear stress indicated that the bioreactor provides homogeneous and reproducible laminar flow conditions with flow rates ranging from 1.48 ml min^{-1} to 47 ml s^{-1}. The bioreactor system can be used to mimic both low and high shear stresses up to approximately 11.2 dyn cm^{-2}. The system was tested using HUVECs, which are directly exposed to blood flow shear stresses *in vivo*. Cytotoxicity tests demonstrated that HUVECs retained a high viability after they were exposed to 1.48 ml min^{-1} flow within the bioreactor system for 24 h. The HUVECs showed a round morphology and no alignment occurred after the dynamic culture. This

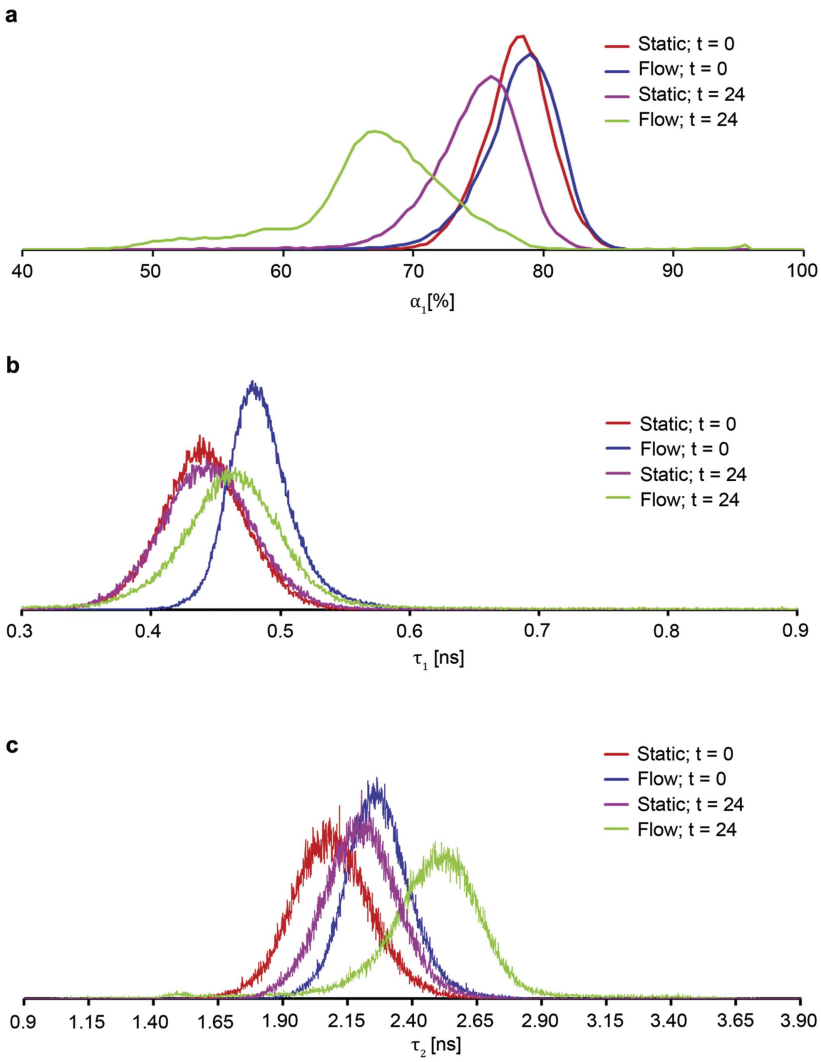

Figure 5. Histograms of (a) the relative contribution of free NAD(P)H (α_1), fluorescence lifetimes of the (b) free (τ_1) and (c) protein-bound (τ_2) NAD(P)H in HUVECs cultured under static or flow conditions.

is in accordance with a previous study, in which Chiu *et al* observed similar characteristics of HUVECs after exposure to a defined shear stress of approximately 0.5 dyn cm^{-2} [40]. In this study, HUVECs were round in shape with random actin filaments located mainly at the periphery of the cells [40]. In contrast, when exposing HUVECs to a relatively high shear stress (20 dyn cm^{-2}), the cells showed an elongated morphology and alignment with the direction of flow [40].

Here, the migration behavior of HUVECs was assessed under static and continuous flow conditions employing a scratch assay in real-time within the bioreactor system. The influence of high and disturbed shear stress on HUVEC migration has been controversially discussed as endothelial migration responses vary depending on the duration and type of applied shear stress [1, 41, 42]. For example, when HUVECs were preconditioned with a relatively high stress of 15 dyn cm^{-2} and then scratched, the migration was inhibited when compared with the static controls [1]. In contrast, when HUVECs were scratched without preconditioning and then cultured with approximately the same conditions (17 dyn cm^{-2}), the migration was increased compared with the static controls [40, 41]. In our study, we observed a low shear stress-induced reduction in migration of HUVECs when compared with the static conditions.

2P-FLIM was utilized to investigate the metabolic activity of HUVECs cultured under low shear stress conditions with the aim to show the suitability of the bioreactor for real-time high-resolution imaging. Kim *et al* have shown that shear stress can alter metabolism in endothelial cells from glycolysis to oxidative phosphorylation-dependent mechanisms [43]. Our data is consistent with these findings as we detected decreased α_1 in 24 h laminar-sheared HUVECs when compared with the static controls or with cells before expose to shear ($t = 0$). This indicates a metabolic switch from glycolysis to oxidative phosphorylation [44]. One possible explanation for this metabolic switch is that laminar shear stress induces apoptosis of endothelial cells by reducing glucose uptake (glycolysis) [45]. A relation between metabolic phenotypes and fluorescence lifetimes of NAD(P)H has been previously reported

[44, 46]. We also observed an increased τ_2 that may correlate to the elevated level of oxidative phosphorylation. Others have suggested that τ_1 is associated with the cytosolic acidification in cells [47]. Interestingly, a previous study has shown that laminar shear stress induces intracellular acidification in endothelial cells [48]. The pH value changes may act as a signaling mechanism for flow-induced changes in endothelial cell metabolism [48]. Therefore, it is possible that the metabolic shifts in laminar-sheared HUVECs are regulated via pH value changes.

In our study, we showed that our newly designed bioreactor system can control shear stress stimulation parameters while allowing visualization and quantification of cell migration and cell–cell interaction under shear stress-stimulated conditions. As this bioreactor system has been designed to also house 3D substrates, such as cell-populated electrospun scaffolds or hydrogels, a future application of this bioreactor system is to study cell-biomaterial interactions. Recently, it was shown that the combination of electrospun scaffolds with shear stress resulted in the increased maturation of induced-pluripotent stem cells-derived smooth muscle cells [49]. With the here presented next generation bioreactor system, simultaneous real-time monitoring and contact-free cell state analyses are now additionally possible. Moreover, due to the combination of bioreactor technology and imaging, the system can also be used in the future for direct cell manipulation such as optoporation and optical reprogramming with the ability to quantify expression, subcellular location and trafficking of receptors in living cells as seen in previous studies [50, 51]. Other potential applications of this bioreactor system have broad implications especially with the recent advances in gene editing. For example, fluorescence-reporter genes could be monitored *in vitro* using this bioreactor system. This real-time monitoring would help uncover mechanisms of disease in order to improve treatments and gain mechanistic knowledge. The ability to modulate the physical parameters such as shear stress and oxygen content could play an important role in cardiovascular tissue engineering and coagulation studies. Real-time monitoring of cells could give insight into the progression and mechanism of disease, which is vital for the advancement of treatment and knowledge in the field of tissue engineering and biomaterials design.

Conclusion

The newly designed flow bioreactor system presented in this study enables the exposure of cells and 3D tissues to shear stress while allowing simultaneous real-time contact-free analyses. We demonstrated that the system is capable of providing reproducible laminar flow in a wide flow range. It is biocompatible, easy-to-use and compatible with a wide range of microscope systems. To prove the functionality of the bioreactor system, we cultured HUVECs under low shear stress conditions for 24 h. Future studies will focus on a systematic study of a long-term culture of HUVECs under various types and magnitudes of shear stresses. Future possibilities for this bioreactor range from observing *in vitro* cell development, including but not limited to direct cell reprogramming or stem cell differentiation, and real-time monitoring of cellular (micro)environments, cell-biomaterial interactions or cellular metabolic changes due to drug applications.

Acknowledgments

The authors thank Pirmin Lakner, Katarina Klett and Simone Liebscher (University Women's Hospital Tübingen) for their support with imaging and cell cultures. This work was funded by the Fulbright US Student Program (JAR), RISE DAAD (ZD), the Ministry of Science, Research and the Arts of Baden-Württemberg (33-729.55-3/214 and SI-BW 01222-91 to KS-L), and the Deutsche Forschungsgemeinschaft (INST 2388/30-1, INST 2388/34-1, SCHE 701/7-1, SCHE 701/10-1 to KS-L).

Disclosure statement

No competing financial interests exist.

ORCID iDs

Katja Schenke-Layland https://orcid.org/0000-0001-8066-5157

References

[1] Tressel S L *et al* 2007 Laminar shear inhibits tubule formation and migration of endothelial cells by an angiopoietin-2-dependent mechanism *Arterioscler. Thromb. Vasc. Biol.* **27** 2150
[2] Wang Y-K and Chen C S 2013 Cell adhesion and mechanical stimulation in the regulation of mesenchymal stem cell differentiation *Int. J. Mol. Cell Med.* **17** 823
[3] Brafman D A 2013 Constructing stem cell microenvironments using bioengineering approaches *Physiol. Genomics* **45** 1123
[4] Kshitiz *et al* 2012 Control of stem cell fate and function by engineering physical microenvironments *Integr. Biol.* **4** 1008
[5] Mammoto T and Ingber D E 2010 Mechanical control of tissue and organ development *Development* **137** 1407
[6] Kaazempur Mofrad M R *et al* 2005 Exploring the molecular basis for mechanosensation, signal transduction, and cytoskeletal remodeling *Acta Biomater.* **1** 281
[7] Grayson W L *et al* 2009 Biomimetic approach to tissue engineering *Semin. Cell Dev. Biol.* **20** 665
[8] Minteer D M, Gerlach J C and Marra K G 2014 Bioreactors addressing diabetes mellitus *J. Diabetes Sci. Technol.* **8** 1227
[9] Mousoulis C *et al* 2013 Single cell spectroscopy: noninvasive measures of small-scale structure and function *Methods* **64** 119
[10] Haagensen J A, Regenberg B and Sternberg C 2011 Advanced microscopy of microbial cells *Adv. Biochem. Eng. Biotechnol.* **124** 21–54

[11] Lakner P H *et al* 2017 Applying phasor approach analysis of multiphoton FLIM measurements to probe the metabolic activity of three-dimensional *in vitro* cell culture models *Sci. Rep.* **7** 42730
[12] Hinderer S *et al* 2015 *In vitro* elastogenesis: instructing human vascular smooth muscle cells to generate an elastic fiber-containing extracellular matrix scaffold *Biomed. Mater.* **10** 034102
[13] Wang C *et al* 2013 Endothelial cell sensing of flow direction *Arterioscler. Thromb. Vasc. Biol.* **33** 2130
[14] Bhatia S N and Ingber D E 2014 Microfluidic organs-on-chips *Nat. Biotechnol.* **32** 760
[15] Niehorster T *et al* 2016 Multi-target spectrally resolved fluorescence lifetime imaging microscopy *Nat. Methods* **13** 257
[16] Sun Y *et al* 2012 Monitoring protein interactions in living cells with fluorescence lifetime imaging microscopy *Methods Enzymol.* **504** 371
[17] Cahalan M D *et al* 2002 Two-photon tissue imaging: seeing the immune system in a fresh light *Nat. Rev. Immunol.* **2** 872
[18] Cubeddu R *et al* 2002 Time-resolved fluorescence imaging in biology and medicine *J. Phys. D: Appl. Phys.* **35** R61
[19] Sanders R *et al* 1995 Quantitative pH imaging in cells using confocal fluorescence lifetime imaging microscopy *Anal. Biochem.* **227** 302
[20] Szmacinski H, Gryczynski I and Lakowicz J R 1996 Three-photon induced fluorescence of the calcium probe Indo-1 *Biophys. J.* **70** 547
[21] Szmacinski H and Lakowicz J R 1997 Sodium green as a potential probe for intracellular sodium imaging based on fluorescence lifetime *Anal. Biochem.* **250** 131
[22] Gerritsen H C *et al* 1997 Fluorescence lifetime imaging of oxygen in living cells *J. Fluorescence* **7** 11
[23] Murata S, Herman P and Lakowicz J R 2001 Texture analysis of fluorescence lifetime images of nuclear DNA with effect of fluorescence resonance energy transfer *Cytometry* **43** 94
[24] Hinderer S *et al* 2014 Engineering of a bio-functionalized hybrid off-the-shelf heart valve *Biomaterials* **35** 2130
[25] Monaghan M G *et al* 2016 Enabling multiphoton and second harmonic generation imaging in paraffin-embedded and histologically stained sections *Tissue Eng.* C **22** 517
[26] Liu M *et al* 2014 Instrument response standard in time-resolved fluorescence spectroscopy at visible wavelength: quenched fluorescein sodium *Appl. Spectrosc.* **68** 577
[27] Luchowski R *et al* 2009 Instrument response standard in time-resolved fluorescence *Rev. Sci. Instrum.* **80** 033109
[28] Sun Y, Day R N and Periasamy A 2011 Investigating protein–protein interactions in living cells using fluorescence lifetime imaging microscopy *Nat. Protocols* **6** 1324
[29] Georgakoudi I and Quinn K P 2012 Optical imaging using endogenous contrast to assess metabolic state *Annu. Rev. Biomed. Eng.* **14** 351
[30] Scott T G *et al* 1970 Synthetic spectroscopic models related to coenzymes and base pairs: V. Emission properties of NADH. Studies of fluorescence lifetimes and quantum efficiencies of NADH, AcPyADH, [reduced acetylpyridineadenine dinucleotide] and simplified synthetic models *J. Am. Chem. Soc.* **92** 687
[31] Jonkman J E *et al* 2014 An introduction to the wound healing assay using live-cell microscopy *Cell Adhes. Migr.* **8** 440
[32] Rangarajan S, Madden L and Bursac N 2014 Use of flow, electrical, and mechanical stimulation to promote engineering of striated muscles *Ann. Biomed. Eng.* **42** 1391
[33] Zhao F and Ma T 2005 Perfusion bioreactor system for human mesenchymal stem cell tissue engineering: dynamic cell seeding and construct development *Biotechnol. Bioeng.* **91** 482
[34] Price A P *et al* 2010 Development of a decellularized lung bioreactor system for bioengineering the lung: the matrix reloaded *Tissue Eng.* A **16** 2581
[35] Kensah G *et al* 2011 A novel miniaturized multimodal bioreactor for continuous *in situ* assessment of bioartificial cardiac tissue during stimulation and maturation *Tissue Eng.* C **17** 463
[36] Bachmann B J *et al* 2016 A novel bioreactor system for the assessment of endothelialization on deformable surfaces *Sci. Rep.* **6** 38861
[37] Wang D *et al* 2010 A stretching device for imaging real-time molecular dynamics of live cells adhering to elastic membranes on inverted microscopes during the entire process of the stretch *Integr. Biol.* **2** 288
[38] Sim J Y *et al* 2012 Uniaxial cell stretcher enables high resolution live cell imaging *2012 IEEE 25th Int. Conf. on Micro Electro Mechanical Systems (MEMS)*
[39] Huang L, Mathieu P S and Helmke B P 2010 A stretching device for high-resolution live-cell imaging *Ann. Biomed. Eng.* **38** 1728
[40] Chiu J-J and Chien S 2011 Effects of disturbed flow on vascular endothelium: pathophysiological basis and clinical perspectives *Physiol. Rev.* **91** 327
[41] Hsu P-P *et al* 2001 Effects of flow patterns on endothelial cell migration into a zone of mechanical denudation *Biochem. Biophys. Res. Commun.* **285** 751
[42] Tardy Y *et al* 1997 Shear stress gradients remodel endothelial monolayers *in vitro* via a cell proliferation-migration-loss cycle *Arterioscler. Thromb. Vasc. Biol.* **17** 3102
[43] Kim B *et al* 2014 Exercise-mediated wall shear stress increases mitochondrial biogenesis in vascular endothelium *PLoS One* **9** e111409
[44] Meleshina A V *et al* 2016 Probing metabolic states of differentiating stem cells using two-photon FLIM *Sci. Rep.* **6** 21853
[45] Doddaballapur A *et al* 2015 Laminar shear stress inhibits endothelial cell metabolism via KLF2-mediated repression of PFKFB3 *Arterioscler. Thromb. Vasc. Biol.* **35** 137
[46] Blacker T S *et al* 2014 Separating NADH and NADPH fluorescence in live cells and tissues using FLIM *Nat. Commun.* **5** 3936
[47] Damalakiene L *et al* 2016 Fluorescence-lifetime imaging microscopy for visualization of quantum dots' endocytic pathway *Int. J. Mol. Cell Med.* **17** 473
[48] Ziegelstein R C, Cheng L and Capogrossi M C 1992 Flow-dependent cytosolic acidification of vascular endothelial cells *Science* **258** 656
[49] Eoh J H *et al* 2017 Enhanced elastin synthesis and maturation in human vascular smooth muscle tissue derived from induced-pluripotent stem cells *Acta Biomater.* **52** 49
[50] Perrio C, Nicole O and Buisson A 2017 GluN2B subunit labeling with fluorescent probes and high-resolution live imaging *Methods Mol. Biol.* **1677** 171
[51] Ribas J *et al* 2016 Cardiovascular organ-on-a-chip platforms for drug discovery and development *Appl. In Vitro Toxicol.* **2** 82
[52] Nava M M, Raimondi M T and Pietrabissa R 2013 A multiphysics 3D model of tissue growth under interstitial perfusion in a tissue-engineering bioreactor *Biomech. Model Mechanobiol.* **12** 1169